Editors' Suggestion

Kinetic Theory of Motility Induced Phase Separation for Active Brownian Particles

Rodrigo Soto,[1] Martín Pinto,[1] and Ricardo Brito[2]
[1]Departamento de Física, FCFM, Universidad de Chile, Santiago, Chile
[2]Departamento de Estructura de la Materia, Física Térmica y Electrónica and GISC, Universidad Complutense de Madrid, Spain

(Received 27 January 2024; accepted 22 April 2024; published 16 May 2024)

When two active Brownian particles collide, they slide along each other until they can continue their free motion. For persistence lengths much larger than the particle diameter, the directors do not change, but the collision can be modeled as producing a net displacement on the particles compared to their free motion in the absence of the encounter. With these elements, a Boltzmann-Enskog-like kinetic theory is built. A linear stability analysis of the homogeneous state predicts a density instability resulting from the effective velocity reduction of tagged particles predicted by the theory.

DOI: 10.1103/PhysRevLett.132.208301

Introduction.—Noninertial self-propelled active particles, even when the dominant interaction between particles is purely repulsive, have a natural tendency to cluster [1–8]. Qualitatively, the mechanism is quite simple. When two particles meet, they remain in contact for a finite time, during which they point in roughly constant directions. If the particle density ρ is high enough, during the time they remain in contact and before one of them changes its direction and escapes, more particles can arrive, becoming the seed of a cluster. That is, clustering is a direct consequence of persistence in motion and excluded volume. Active Brownian particles (ABPs) [9–11] are an ideal model to test this hypothesis. Here, particles move persistently at constant speed V along directors that change slowly by rotational diffusion with coefficient D_r, and interact only by excluded volume. The equations of motion for the position $\mathbf{r}_i$ and the director $\hat{\mathbf{n}}_i$ of the particle i are

$$\dot{\mathbf{r}}_i = V\hat{\mathbf{n}}_i + \mathbf{F}_i, \qquad \dot{\hat{\mathbf{n}}}_i = \sqrt{2D_r}\boldsymbol{\xi}_i(t) \times \hat{\mathbf{n}}_i, \qquad (1)$$

where $\boldsymbol{\xi}_i$ are uncorrelated white noises and $\mathbf{F}_i$ the hard-core interparticle force acting on i. For the case of spherical ABPs with diameter σ, despite the absence of interparticle attraction, persistence was indeed found to induce clustering [3,4,8]. Dimensional analysis and simulations indicate that the relevant control parameters in d spatial dimensions are $\tilde{\rho} = \rho\sigma^d$ (which is proportional to the volume fraction) and the persistence length $\ell = V/(\sigma D_r)$, also called the active Péclet number. Clustering takes place for high $\tilde{\rho}$ and ℓ [4,8,12–14].

A theoretical framework to describe the clustering instability is the so-called motility induced phase separation (MIPS), which states that the effective particle velocities are reduced due to particle encounters, which turn out to be a decreasing function of the local density $V_{\text{eff}}(\rho)$ [15,16]. Then, if fluctuations create a density excess in a particular region, the particles there will move at a lower speed, implying that the incoming diffusive particle flux will be greater than the outgoing one, creating a mechanism for instability. This model allows for a hydrodynamiclike description of the density and polarization fields, where it has been shown that in the limit of very large ℓ the density mode becomes unstable akin to spinodal decomposition if $-(\partial V_{\text{eff}}/\partial\rho) > V_{\text{eff}}/\rho$, that is, if the velocity reduction is sufficiently drastic [15,16]. For finite persistence lengths, corrections to this prediction appear, and the instability develops only for ℓ greater than a threshold, in agreement with simulations [16]. Nonequilibrium thermodynamic formulations allow one to obtain the binodal curves besides the spinodals [16–20].

Microscopically, the MIPS instability has been derived for lattice models, where it is possible to write the system dynamics in terms of a master equation [2]. With the usual approximation of no correlations, MIPS is predicted to occur for analogous conditions as for ABPs. For ABPs, the MIPS explanation is realized by noting that hard-core collisions cause particles to take longer to travel a distance, i.e., the effective velocity is reduced by collisions. In Ref. [21], for large spatial dimensions, $d \gg 1$, a kinetic-theoretic analysis allowed to compute the effective velocity reduction, obtaining $V_{\text{eff}} = V(1-\rho/\rho_{\text{cr}})$, where ρ_{cr} is a characteristic density that depends on d. Also, using a mean-field approximation, the same dependence for V_{eff} was found for ABP, although no analytical derivation of ρ_{cr} was made [22]. In Ref. [23], hydrodynamic equations showing MIPS were derived from a mean-field kinetic theory for inertial ABPs.

Despite its importance, a complete microscopic derivation of MIPS for ABPs has not yet been obtained. Here, we present a kinetic theory description of ABPs in the large persistence regime, from which we derive the conditions for MIPS to occur with a clear and identifiable mechanism for the reduction of the effective velocity. Kinetic theory is a powerful tool to coarse-grain microscopic models to obtain macroscopic equations for a reduced number of relevant fields (hydrodynamiclike equations) [24]. In the

case of active matter, kinetic equations have been successfully used in the low density limit for active particles presenting short-range aligning interactions [25–30]. For microswimmers moving in a fluid the interactions are mediated by the fluid and become long-range. In this case, a mean-field approximation, analogous to that used in plasma physics, has been used to study the instabilities that appear in these suspensions [31,32] and the effects of fluctuations [33]. Also, a kinetic analysis of the interactions of the swimmers with the fluid and among themselves has been used to characterize the rheology of bacterial suspensions [34,35]. The case of ABP is more challenging for the construction of a kinetic theory because the interactions are short-ranged, but due to persistence, particles remain in contact for finite time and the usual concept of a collision is difficult to visualize. Here, however, we show that it is indeed possible to formulate a kinetic description of ABPs at moderate densities and large ℓ, with collision events having well-defined pre and postcollisional states. The kinetic equation will be presented in general for d spatial dimensions, but the explicit calculations will be performed in two dimensions. Finally, we want to emphasize that ABPs have become a prototype for active matter because of their theoretical simplicity, the possibility to perform efficient simulations, and because, besides showing clustering, this model accurately describes the properties of many experimental realizations of noninertial active matter such as Janus colloids [7,36–38], Quincke rollers [39,40], or active droplets [41], just to name a few. The construction of a kinetic theory for ABPs has, therefore, the possibility to help with the theoretical description of different phenomena shown by active matter.

Effective collision theory for active Brownian particles.—When two ABPs meet, steric repulsion prevents them from continuing their free motion and they begin to slide in contact with each other. That is represented in Fig. 1: two particles moving with velocity directors $\hat{\mathbf{n}}_1$ and $\hat{\mathbf{n}}_2$, get in contact at positions marked by light yellow and light green disks. They start to slide around each other until they can detach again, indicated with dark yellow and dark green disks. Such condition is mathematically satisfied when $(\hat{\mathbf{n}}_1 - \hat{\mathbf{n}}_2) \cdot (\mathbf{r}_1 - \mathbf{r}_2) = 0$, being $\mathbf{r}_i$ the position of the particle $i = 1, 2$. Trajectories displayed by solid black lines, while dotted lines would be the trajectories without the collision. The duration of this collision process t_{col} is of the order of σ/V. Then, in the regime of large persistence lengths, $\ell \gg 1$, the directors have hardly changed, allowing us to make the approximation that the directors remain constant in the process. What changes are the particle positions. If we call $\mathbf{r}_i^{\mathrm{ini}}$ the particle positions when they first meet, $\mathbf{r}_i^{\mathrm{end}}$ the positions when they depart, and $\boldsymbol{\Delta}_i^0 = V\hat{\mathbf{n}}_i t_{\mathrm{col}}$, the distance traveled if the collision had not occurred, a collision results in net displacements $\boldsymbol{\Delta}_i = \mathbf{r}_i^{\mathrm{end}} - \mathbf{r}_i^{\mathrm{ini}} - \boldsymbol{\Delta}_i^0$. Then, a collision can be modeled as an instantaneous process where the directors do not change, but the positions change as $\mathbf{r}_i \to \mathbf{r}_i + \boldsymbol{\Delta}_i$ (depicted in Fig. 1).

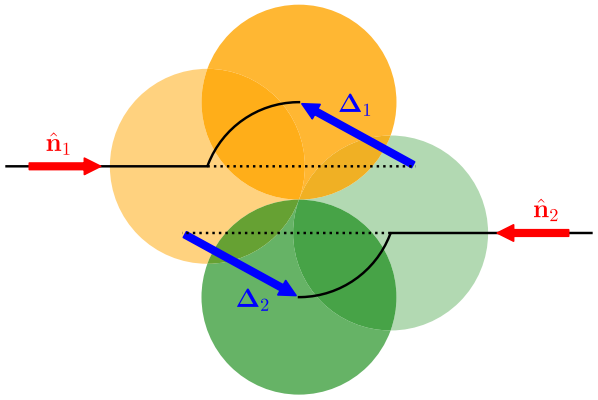

FIG. 1. Scheme of an effective collision for particles 1 (orange) and 2 (green). Directors $\hat{\mathbf{n}}_{1,2}$ are indicated by red arrows. The light colored circles show the initial state of the collision, while the dark colored circles show the state when the particles start to depart. The solid black lines show the actual trajectories up to the point of departure. The trajectories that the particles would had have followed without the collision are shown as black dotted lines. Finally, blue arrows show the effective displacements $\boldsymbol{\Delta}_{1,2}$ caused by the collision. For simplicity, the figure only shows the case where $\hat{\mathbf{n}}_2 = -\hat{\mathbf{n}}_1$, in which case the center of mass remains fixed.

It is possible to find an explicit expression for the displacements in terms of the particle directors and the unit vector $\hat{\boldsymbol{\sigma}}$ pointing from particle 1 to 2 at the beginning of the collision. The calculation (see the Supplemental Material [42]) consists of solving the equation of motion of the two particles with an additional normal force to maintain the impenetrability condition. The results are that $t^{\mathrm{col}} = \sigma/[V|\hat{\mathbf{n}}_2 - \hat{\mathbf{n}}_1|] \log|\tan(\theta/2)|$, with θ the angle between $\hat{\boldsymbol{\sigma}}$ and $\hat{\mathbf{n}}_2 - \hat{\mathbf{n}}_1$, and

$$\boldsymbol{\Delta}_1 = -\boldsymbol{\Delta}_2 = -\sigma\frac{\hat{\boldsymbol{\sigma}}_{\mathrm{end}} - \hat{\boldsymbol{\sigma}}}{2} - V\Delta t^{\mathrm{col}}\frac{\hat{\mathbf{n}}_1 - \hat{\mathbf{n}}_2}{2}, \tag{2}$$

$$= -\frac{\sigma}{2}\left[\hat{\boldsymbol{\sigma}}_{\mathrm{end}} - \hat{\boldsymbol{\sigma}} - \log|\tan(\theta_0/2)|\frac{\hat{\mathbf{n}}_1 - \hat{\mathbf{n}}_2}{|\hat{\mathbf{n}}_2 - \hat{\mathbf{n}}_1|}\right]. \tag{3}$$

Here, $\hat{\boldsymbol{\sigma}}_{\mathrm{end}}$ is the unit vector from 1 to 2 at the end of the collision, which is in the same plane as $\hat{\boldsymbol{\sigma}}$ and $(\hat{\mathbf{n}}_2 - \hat{\mathbf{n}}_1)$, and perpendicular to the latter. Note that although the system does not obey Galilean invariance, the displacements for the colliding particles are reciprocal. The collision time t^{col} diverges for head-on collisions ($\theta = \pi$), but it is an integrable divergence, giving finite results for the relevant calculations below.

Average velocity reduction.—For a tagged particle, the displacement has a component perpendicular to its director that contributes to diffusion and mixing. More importantly for the purpose of understanding MIPS, there is a component parallel to the director $\Delta_{\parallel} = \boldsymbol{\Delta}_1 \cdot \hat{\mathbf{n}}_1$, which we show

below to be negative on average. Therefore, the effective particle velocity is reduced as a result of collisions.

Before proceeding to derive the full kinetic theory, we present some elements of the theory by computing in a homogeneous system the average parallel displacement rate due to collisions, $\langle d\Delta_\parallel/dt|_{\rm coll}\rangle$. Let $i=1$ be the tagged particle. For the collisions with particle 2, we assume the molecular chaos hypothesis for the precollisional states, corrected with the static pair correlation function at contact χ, as in the Enskog theory for moderately dense gases. That is, the collision rate for the two particles is $\chi(\rho)f(\hat{\mathbf{n}}_1)f(\hat{\mathbf{n}}_2)|V\sigma^{d-1}(\hat{\mathbf{n}}_2-\hat{\mathbf{n}}_1)\cdot\hat{\boldsymbol{\sigma}}|\Theta[-(\hat{\mathbf{n}}_2-\hat{\mathbf{n}}_1)\cdot\hat{\boldsymbol{\sigma}}]$, where f is the distribution function. The factor in absolute value represents the collision rate, which is proportional to the velocity V multiplied by the effective cross section. Finally, Θ is the Heaviside step function to select particles that are approaching [24]. Assuming an equilibrium distribution in two dimensions, $f(\hat{\mathbf{n}})=\rho/(2\pi)$, after integrating over all directions of $\hat{\mathbf{n}}_2$ and $\hat{\boldsymbol{\sigma}}$, we obtain $\langle d\Delta_\parallel/dt|_{\rm coll}\rangle=-\rho\chi\pi\sigma^2V/4$ (see the Supplemental Material), which, as anticipated, is negative, indicating that collisions reduce the effective velocity of a particle to

$$V_{\rm eff}=V(1-\rho\chi\pi\sigma^2/4). \tag{4}$$

The spinodal density ρ^* for the MIPS instability is given by the condition $-(\partial V_{\rm eff}/\partial\rho)=V_{\rm eff}/\rho$ [15,16], which upon substitution of Eq. (4) reads

$$\rho^*\sigma^2[\chi(\rho^*)+\rho^*\chi'(\rho^*)/2]=2/\pi, \tag{5}$$

with $\chi'=d\chi/d\rho$, assuming that χ depends on the local density. To evaluate Eq. (5), it is necessary to know the value of χ, but it has not been determined for ABPs [43]. Therefore, we have to rely on expressions valid for elastic, passive particles. The first approach can be to neglect correlations, $\chi=1$, approximation valid for very low densities. In this case, Eq. (5) gives $\rho^*\sigma^2=2/\pi\approx0.64$, which is quite large, in the range of high densities and near close packing, $\rho_{\rm max}=2/(\sqrt{3}\sigma^2)$. Then, the assumption of no correlations is hard to justify. It is then necessary to use an expression for χ valid at moderate densities, such as that of Ref. [47], for hard disks in equilibrium $\chi_{\rm hd}=(1-7\pi\rho\sigma^2/64)/(1-\pi\rho\sigma^2/4)^2$. With this expression, the spinodal density is $\rho^*\sigma^2\approx0.32$ (area fraction $\phi^*=\pi\rho^*\sigma^2/4\approx0.25$), which is in the region of moderate densities where $\chi_{\rm hd}$ is expected to be valid. The comparison with the simulation results for the spinodal curves is excellent. Simulations of ABPs with hard disk interactions, Refs. [13,48,49], predict $\phi^*\approx0.25$ for infinitely large ℓ. Other authors carry out simulations for ABPs interacting with softer potentials (see, e.g., Refs. [12,14,50]) predicting $\phi^*\approx0.30$–0.35. Softer potentials delay the MIPS transition, that is, the spinodal line moves to higher densities [51,52]. In both cases the agreement with our theory is excellent.

Kinetic theory.—A kinetic theory that can be analyzed more formally to study MIPS can be derived following the ideas presented above. In absence of collisions, the distribution function evolves purely by the effects of free particle motion and rotational diffusion. Collisions can be included in the kinetic equation in a complete analogy to the Boltzmann-Enskog equation for moderately dense gases, except that instead of changing velocities, here each collision has the effect of displacing particles by an amount $\boldsymbol{\Delta}_i$. Thus the equation for $f(\mathbf{r}_1,\hat{\mathbf{n}}_1,t)$ reads

$$\frac{\partial f}{\partial t}+V\hat{\mathbf{n}}_1\cdot\frac{\partial}{\partial\mathbf{r}_1}f=D_{\rm r}\nabla^2_{\hat{\mathbf{n}}_1}f+J[f]. \tag{6}$$

The first three terms, up to the Laplace-Beltrami operator $\nabla^2_{\hat{\mathbf{n}}_1}$, are standard to account for the free streaming and rotational diffusion of the particles [9–11,26,30,31,34]. The collisional term J we propose is written, as in the Boltzmann-Enskog equation, as the difference of a gain and a loss term,

$$\begin{aligned}J[f]=\int\chi\left(\rho\left(\frac{r_1'+r_2'}{2}\right)\right)&f(\mathbf{r}_1',\hat{\mathbf{n}}_1)f(\mathbf{r}_2',\hat{\mathbf{n}}_2)\\&\times|V\sigma^{d-1}(\hat{\mathbf{n}}_2-\hat{\mathbf{n}}_1)\cdot\hat{\boldsymbol{\sigma}}|\Theta[-(\hat{\mathbf{n}}_2-\hat{\mathbf{n}}_1)\cdot\hat{\boldsymbol{\sigma}}]\delta(\mathbf{r}_2'-\mathbf{r}_1'-\sigma\hat{\boldsymbol{\sigma}})\\&\times[\delta(\mathbf{r}_1-\mathbf{r}_1'-\boldsymbol{\Delta}_1)-\delta(\mathbf{r}_1-\mathbf{r}_1')]d\mathbf{r}_1'd\mathbf{r}_2'd\hat{\mathbf{n}}_2d\hat{\boldsymbol{\sigma}}.\end{aligned} \tag{7}$$

The loss term, with the factor $\delta(\mathbf{r}_1-\mathbf{r}_1')$, indicates that a particle with position $\mathbf{r}_1$ and director $\hat{\mathbf{n}}_1$ collides with a partner at the previously given rate, resulting in a decrease of $f(\mathbf{r}_1,\hat{\mathbf{n}}_1,t)$. The gain term, with the factor $\delta(\mathbf{r}_1-\mathbf{r}_1'-\boldsymbol{\Delta}_1)$ accounts for the increase in $f(\mathbf{r}_1,\hat{\mathbf{n}}_1,t)$ due to a particle located at $\mathbf{r}_1-\boldsymbol{\Delta}_1$ colliding with a partner such that after the collision it ends at $\mathbf{r}_1$ with director $\hat{\mathbf{n}}_1$. Both collision terms have the factor χ evaluated at the middle position of the two colliding particles.

The subtraction of the two Dirac deltas in Eq. (7) represents the instantaneous particle teleportation at collisions, concept that is at the basis of the effective collision theory presented here. It is for the mass, the equivalent of the collisional transfer of momentum and energy for hard sphere systems, where these quantities are instantaneously exchanged between particles in a collision. As noted by Irving and Kirkwood, collisional transfers imply that momentum and energy are not locally conserved. However, by assuming that the momentum and energy flow along the line connecting the particle centers, it is possible to define local stress tensors and heat fluxes [24,53]. Here, we proceed analogously. For that, we note that we can write $\delta(\mathbf{r}-\mathbf{r}_a)-\delta(\mathbf{r}-\mathbf{r}_b)=-\nabla_\alpha\int_{\mathbf{r}_a}^{\mathbf{r}_b}\delta(\mathbf{r}-\mathbf{s})ds_\alpha$, where summation over repeated indices is used. With this expression, the collision term can be written as a divergence of a vector field, denoted by $\mathbf{G}(\mathbf{r},\hat{\mathbf{n}},t)$, with the form

$$J[f] = -\nabla_\alpha G_\alpha(\mathbf{r}_1, \hat{\mathbf{n}}_1, t) = -\nabla_\alpha \Bigg[\int \chi\left(\rho\left(\frac{r_1' + r_2'}{2}\right)\right) \times f(\mathbf{r}_1', \hat{\mathbf{n}}_1) f(\mathbf{r}_2', \hat{\mathbf{n}}_2) |V\sigma^{d-1}(\hat{\mathbf{n}}_2 - \hat{\mathbf{n}}_1)\cdot\hat{\boldsymbol{\sigma}}| \Theta[-(\hat{\mathbf{n}}_2 - \hat{\mathbf{n}}_1)\cdot\hat{\boldsymbol{\sigma}}] \times \delta(\mathbf{r}_2' - \mathbf{r}_1' - \sigma\hat{\boldsymbol{\sigma}}) \times \int_{\mathbf{r}_1'}^{\mathbf{r}_1'+\boldsymbol{\Delta}_1} \delta(\mathbf{r}_1 - \mathbf{s}) ds_\alpha d\mathbf{r}_1' d\mathbf{r}_2' d\hat{\mathbf{n}}_2 d\hat{\boldsymbol{\sigma}} \Bigg]. \tag{8}$$

With this expression, integrating Eq. (6) over $\hat{\mathbf{n}}_1$ gives the mass conservation equation

$$\frac{\partial \rho}{\partial t} = -\nabla \cdot \mathbf{J}, \tag{9}$$

where

$$\rho(\mathbf{r}, t) = \int f(\mathbf{r}, \hat{\mathbf{n}}, t) d\hat{\mathbf{n}}, \tag{10}$$

$$\mathbf{J}(\mathbf{r}, t) = V \int f(\mathbf{r}, \hat{\mathbf{n}}, t)\hat{\mathbf{n}}\, d\hat{\mathbf{n}} + \int \mathbf{G}(\mathbf{r}, \hat{\mathbf{n}}, t) d\hat{\mathbf{n}} \tag{11}$$

are the density and the mass flux vector, respectively.

Linear perturbation and MIPS.—Having derived the kinetic equation for ABPs, we now proceed to study the stability of the homogeneous state to determine if MIPS is well described by this theory. For simplicity, we consider the two-dimensional case. First, it is easy to verify by direct substitution that the homogeneous and isotropic state, described by $f_0 = \rho/(2\pi)$, is a stationary solution of the kinetic equation. Since the kinetic equation is homogeneous in space, we can use spatial Fourier modes for the linear stability analysis. For the $\hat{\mathbf{n}}$ part of f, we consider a series of angular Fourier modes for the distribution of the director. In summary, we study solutions of the form

$$f(\mathbf{r}, \hat{\mathbf{n}}, t) = f_0 + e^{i\mathbf{k}\cdot\mathbf{r} + \lambda t} \sum_m g_m e^{im\phi}, \tag{12}$$

where λ is the rate of amplification ($\mathrm{Re}\lambda > 0$) or decay ($\mathrm{Re}\lambda < 0$) of the perturbation. Projecting back the kinetic equation (6) in the mode $e^{-ip\phi}$ and choosing $\mathbf{k} = k\hat{\mathbf{x}}$, gives the eigenvalue problem for λ,

$$ikV \sum_m I_{pm}(k) g_m - D_r p^2 g_p - \frac{ikV}{2}(g_{p+1} + g_{p-1}) = \lambda g_p, \tag{13}$$

where the matrix elements $I_{pm}(k)$ are given in terms of the displacement $\boldsymbol{\Delta}_1$ (see the Supplemental Material), and the prefactor ik has been explicitly put to reflect the effect of the divergence operator in the collision operator [Eq. (8)]. The eigenvalues λ_n can be obtained with increasing number of angular Fourier modes. Figure 2 shows two cases, one that is stable and one where the real part of an eigenvalue is positive, signaling the appearance of an instability, where the matrices have been truncated to seven modes ($p = -3, -2, \ldots, 3$). For any number of modes, it is found

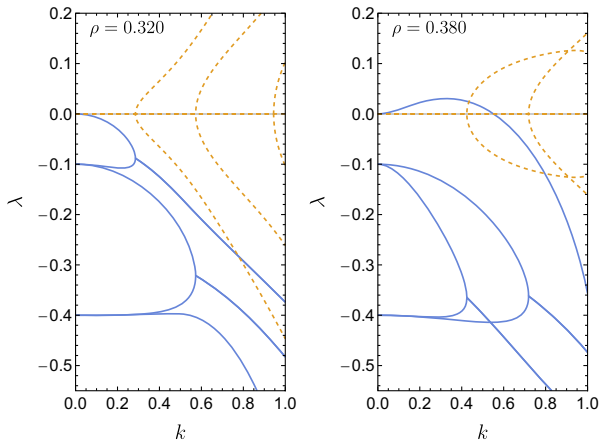

FIG. 2. Dynamical eigenvalues of the first five modes as a function of the wave vector k for $D_r = 0.1$ ($\ell = 10$), $\chi = \chi_{hd}$, and $\rho = 0.32$ (left) and $\rho = 0.38$ (right), obtained by truncating the dynamical matrix to $p = -3, -2, \ldots, 3$. The real (imaginary) parts are shown with solid blue (dashed orange) lines. Units have been chosen so that $V = \sigma = 1$.

that for $k = 0$ the eigenvalues are simply $\lambda_n = -D_r n^2$, meaning that all modes are stable except for one that is marginal, the density mode. For finite but small wave vectors, the real part of the density mode eigenvalue is quadratic in k. Then, for the purpose of this Letter, which is to show that MIPS is predicted by kinetic theory, it is sufficient to show that for small wave vectors the density mode eigenvalue can be positive, analysis that can be done using perturbation theory. For that, a small k expansion of the matrix elements is needed, which can be done analytically using the explicit expression of $\boldsymbol{\Delta}_1$ (see the Supplemental Material). It is found that for $I_{pm}(k = 0)$ the only nonzero elements are when $m = p \pm 1$, with $I_{\pm1,0} = \rho(2\chi + \rho\chi')\pi\sigma^2/8$, $I_{0,\pm1} = 0$, and $I_{p,p\pm1} = \rho\chi\pi\sigma^2/8$ for the rest. Also needed is $dI_{00}(k = 0)/dk = i2\sigma G(2\rho\chi + \rho^2\chi')/\pi$, where $G \approx 0.916$ is the Catalan constant. With these elements, perturbation theory gives $\lambda_0 = (V^2/2D_r)[(\rho\pi\sigma^2/4)(2\chi + \rho\chi')(1 - 16GD_r\sigma/V\pi^2) - 1]k^2 + \mathcal{O}(k^3)$. The spinodal density ρ^* for MIPS is determined by the change of sign of the k^2 coefficient, resulting in a value that grows with D_r. In the limit of large persistence lengths ($D_r \to 0$), where the present theory is valid, ρ^* is obtained from the reduced equation (5). Notably, the spinodal density obtained from the heuristic analysis of the effective velocity reduction coincides with that obtained from the formal analysis of the kinetic equation.

Discussion.—The kinetic theory presented here is expected to be a valid formalism for different regimes occurring in active Brownian particles, and when additional interactions with external fields or between particles are considered. The only limitation is that the persistence length is large and that no long-lived bound states are formed, as happens for example in some nonreciprocal

interactions [54,55]. As usual in kinetic theory, it is necessary to assume absence of all or at least some correlations in the precollisional state. Here, we were able to build the theory assuming that there are no director-director correlations, but that there are position correlations, which were considered in the factor χ. To make more quantitative predictions, it is crucial to evaluate this factor. Note that no assumption has been made about the postcollisional states, which are indeed highly correlated.

The effective collision theory and the associated collision operator were obtained in the limit of infinite persistence lengths. For a more complete theory, it becomes relevant to develop a systematic approach to derive corrections for large but finite persistence lengths, where, as an effect of rotational diffusion, colliding particles can escape at different angles and with new directors, as in the case of tumbling particles in an array of fixed obstacles [56]. Formal methods like those used in Refs. [57,58] can be fruitful for this purpose. Heuristically, nevertheless, it is possible to advance that on average colliding particles will escape earlier for finite persistence lengths. This results in a less pronounced reduction of the effective velocity (4), implying that the spinodal density ρ^* should grow with D_r, consistently with experiments and simulations. This dependence of ρ^* with D_r of kinematic origin should be added to the dependence found above in the linear stability analysis.

The application of the kinetic theory to an initially homogeneous gas correctly predicts MIPS without any *ad hoc* hypothesis about the effective velocity. Rather, its reduction by collisions appears naturally and the predicted spinodal density shows an excellent agreement with the extrapolation of simulations to very large persistence lengths. Finally, for a complete analysis of the phase diagram, with the binodal curves besides the spinodal ones, it would be necessary to solve the stationary long-time nonlinear dynamics of the kinetic equation, which will be the purpose of future work.

This research was supported by the Fondecyt Grant No. 1220536 and Millennium Science Initiative Program NCN19_170D of ANID, Chile. The work of R. B. is supported from Grant No. PID2020-113455GB-I00, Ministerio de Ciencia e Innovación, Spain. R. S. thanks Aparna Baskaran and Andrea Puglisi for inspiring discussions.

[1] H.-P. Zhang, A. Be'er, E.-L. Florin, and H. L. Swinney, Collective motion and density fluctuations in bacterial colonies, Proc. Natl. Acad. Sci. U.S.A. **107**, 13626 (2010).

[2] A. G. Thompson, J. Tailleur, M. E. Cates, and R. A. Blythe, Lattice models of nonequilibrium bacterial dynamics, J. Stat. Mech. (2011) P02029.

[3] Y. Fily and M. C. Marchetti, Athermal phase separation of self-propelled particles with no alignment, Phys. Rev. Lett. **108**, 235702 (2012).

[4] G. S. Redner, M. F. Hagan, and A. Baskaran, Structure and dynamics of a phase-separating active colloidal fluid, Phys. Rev. Lett. **110**, 055701 (2013).

[5] I. Theurkauff, C. Cottin-Bizonne, J. Palacci, C. Ybert, and L. Bocquet, Dynamic clustering in active colloidal suspensions with chemical signaling, Phys. Rev. Lett. **108**, 268303 (2012).

[6] J. Palacci, S. Sacanna, A. P. Steinberg, D. J. Pine, and P. M. Chaikin, Living crystals of light-activated colloidal surfers, Science **339**, 936 (2013).

[7] I. Buttinoni, J. Bialké, F. Kümmel, H. Löwen, C. Bechinger, and T. Speck, Dynamical clustering and phase separation in suspensions of self-propelled colloidal particles, Phys. Rev. Lett. **110**, 238301 (2013).

[8] D. Levis and L. Berthier, Clustering and heterogeneous dynamics in a kinetic Monte Carlo model of self-propelled hard disks, Phys. Rev. E **89**, 062301 (2014).

[9] P. Romanczuk, M. Bär, W. Ebeling, B. Lindner, and L. Schimansky-Geier, Active Brownian particles: From individual to collective stochastic dynamics, Eur. Phys. J. Spec. Top. **202**, 1 (2012).

[10] M. E. Cates and J. Tailleur, When are active Brownian particles and run-and-tumble particles equivalent? Consequences for motility-induced phase separation, Europhys. Lett. **101**, 20010 (2013).

[11] A. P. Solon, M. E. Cates, and J. Tailleur, Active Brownian particles and run-and-tumble particles: A comparative study, Eur. Phys. J. Spec. Top. **224**, 1231 (2015).

[12] Y. Fily, S. Henkes, and M. C. Marchetti, Freezing and phase separation of self-propelled disks, Soft Matter **10**, 2132 (2014).

[13] P. Digregorio, D. Levis, A. Suma, L. F. Cugliandolo, G. Gonnella, and I. Pagonabarraga, Full phase diagram of active Brownian disks: From melting to motility-induced phase separation, Phys. Rev. Lett. **121**, 098003 (2018).

[14] R. Van Damme, J. Rodenburg, R. Van Roij, and M. Dijkstra, Interparticle torques suppress motility-induced phase separation for rodlike particles, J. Chem. Phys. **150**, 164501 (2019).

[15] J. Tailleur and M. E. Cates, Statistical mechanics of interacting run-and-tumble bacteria, Phys. Rev. Lett. **100**, 218103 (2008).

[16] M. E. Cates and J. Tailleur, Motility-induced phase separation, Annu. Rev. Condens. Matter Phys. **6**, 219 (2015).

[17] R. Wittkowski, A. Tiribocchi, J. Stenhammar, R. J. Allen, D. Marenduzzo, and M. E. Cates, Scalar φ^4 field theory for active-particle phase separation, Nat. Commun. **5**, 4351 (2014).

[18] S. C. Takatori and J. F. Brady, Towards a thermodynamics of active matter, Phys. Rev. E **91**, 032117 (2015).

[19] A. P. Solon, J. Stenhammar, M. E. Cates, Y. Kafri, and J. Tailleur, Generalized thermodynamics of phase equilibria in scalar active matter, Phys. Rev. E **97**, 020602(R) (2018).

[20] A. K. Omar, H. Row, S. A. Mallory, and J. F. Brady, Mechanical theory of nonequilibrium coexistence and motility-induced phase separation, Proc. Natl. Acad. Sci. U.S.A. **120**, e2219900120 (2023).

[21] T. A. de Pirey, G. Lozano, and F. Van Wijland, Active hard spheres in infinitely many dimensions, Phys. Rev. Lett. **123**, 260602 (2019).

[22] J. Bialké, H. Löwen, and T. Speck, Microscopic theory for the phase separation of self-propelled repulsive disks, Europhys. Lett. **103**, 30008 (2013).
[23] B. Hancock and A. Baskaran, Statistical mechanics and hydrodynamics of self-propelled hard spheres, J. Stat. Mech. (2017) 033205.
[24] R. Soto, *Kinetic Theory and Transport Phenomena* (Oxford University Press, New York, 2016).
[25] I. S. Aranson and L. S. Tsimring, Pattern formation of microtubules and motors: Inelastic interaction of polar rods, Phys. Rev. E **71**, 050901(R) (2005).
[26] E. Bertin, M. Droz, and G. Grégoire, Boltzmann and hydrodynamic description for self-propelled particles, Phys. Rev. E **74**, 022101 (2006).
[27] A. Baskaran and M. C. Marchetti, Hydrodynamics of self-propelled hard rods, Phys. Rev. E **77**, 011920 (2008).
[28] E. Bertin, M. Droz, and G. Grégoire, Hydrodynamic equations for self-propelled particles: Microscopic derivation and stability analysis, J. Phys. A **42**, 445001 (2009).
[29] T. Ihle, Towards a quantitative kinetic theory of polar active matter, Eur. Phys. J. Spec. Top. **223**, 1293 (2014).
[30] B. Mahault, X.-c. Jiang, E. Bertin, Y.-q. Ma, A. Patelli, X.-q. Shi, and H. Chaté, Self-propelled particles with velocity reversals and ferromagnetic alignment: Active matter class with second-order transition to quasi-long-range polar order, Phys. Rev. Lett. **120**, 258002 (2018).
[31] D. Saintillan and M. J. Shelley, Instabilities and pattern formation in active particle suspensions: Kinetic theory and continuum simulations, Phys. Rev. Lett. **100**, 178103 (2008).
[32] B. Ezhilan, M. J. Shelley, and D. Saintillan, Instabilities and nonlinear dynamics of concentrated active suspensions, Phys. Fluids **25**, 070607 (2013).
[33] Y. Qian, P. R. Kramer, and P. T. Underhill, Stochastic kinetic theory for collective behavior of hydrodynamically interacting active particles, Phys. Rev. Fluids **2**, 043104 (2017).
[34] D. Saintillan, The dilute rheology of swimming suspensions: A simple kinetic model, Exp. Mech. **50**, 1275 (2010).
[35] M. Guzmán and R. Soto, Nonideal rheology of semidilute bacterial suspensions, Phys. Rev. E **99**, 012613 (2019).
[36] W. F. Paxton, K. C. Kistler, C. C. Olmeda, A. Sen, S. K. St. Angelo, Y. Cao, T. E. Mallouk, P. E. Lammert, and V. H. Crespi, Catalytic nanomotors: Autonomous movement of striped nanorods, J. Am. Chem. Soc. **126**, 13424 (2004).
[37] J. Bialké, T. Speck, and H. Löwen, Active colloidal suspensions: Clustering and phase behavior, J. Non-Cryst. Solids **407**, 367 (2015).
[38] F. Ginot, I. Theurkauff, D. Levis, C. Ybert, L. Bocquet, L. Berthier, and C. Cottin-Bizonne, Nonequilibrium equation of state in suspensions of active colloids, Phys. Rev. X **5**, 011004 (2015).
[39] A. Bricard, J.-B. Caussin, N. Desreumaux, O. Dauchot, and D. Bartolo, Emergence of macroscopic directed motion in populations of motile colloids, Nature (London) **503**, 95 (2013).
[40] D. Geyer, D. Martin, J. Tailleur, and D. Bartolo, Freezing a flock: Motility-induced phase separation in polar active liquids, Phys. Rev. X **9**, 031043 (2019).
[41] G. Ramos, M. L. Cordero, and R. Soto, Bacteria driving droplets, Soft Matter **16**, 1359 (2020).
[42] See Supplemental Material at http://link.aps.org/supplemental/10.1103/PhysRevLett.132.208301 for detailed calculations of the displacements, the parametrization of collisions, and the linear stability analysis.
[43] Although the pair distribution function $g(\mathbf{r})$ for ABPs has been measured in Refs. [44,45], it is important to recall that for the kinetic equation, $\chi = \lim_{r\to\sigma^+} g(\mathbf{r})$ must be evaluated only for precollisional states. Otherwise, artificially large values are obtained as reported in Ref. [46].
[44] N. de Macedo Biniossek, H. Löwen, T. Voigtmann, and F. Smallenburg, Static structure of active Brownian hard disks, J. Phys. Condens. Matter **30**, 074001 (2018).
[45] J. Jeggle, J. Stenhammar, and R. Wittkowski, Pair-distribution function of active Brownian spheres in two spatial dimensions: Simulation results and analytic representation, J. Chem. Phys. **152**, 194903 (2020).
[46] R. Soto and M. Mareschal, Statistical mechanics of fluidized granular media: Short-range velocity correlations, Phys. Rev. E **63**, 041303 (2001).
[47] D. Henderson, A simple equation of state for hard discs, Mol. Phys. **30**, 971 (1975).
[48] D. Levis, J. Codina, and I. Pagonabarraga, Active Brownian equation of state: Metastability and phase coexistence, Soft Matter **13**, 8113 (2017).
[49] P. Nie, J. Chattoraj, A. Piscitelli, P. Doyle, R. Ni, and M. P. Ciamarra, Stability phase diagram of active Brownian particles, Phys. Rev. Res. **2**, 023010 (2020).
[50] S. A. Mallory, A. K. Omar, and J. F. Brady, Dynamic overlap concentration scale of active colloids, Phys. Rev. E **104**, 044612 (2021).
[51] J. Martin-Roca, R. Martinez, L. C. Alexander, A. L. Diez, D. G. Aarts, F. Alarcon, J. Ramírez, and C. Valeriani, Characterization of MIPS in a suspension of repulsive active Brownian particles through dynamical features, J. Chem. Phys. **154**, 164901 (2021).
[52] M. Sanoria, R. Chelakkot, and A. Nandi, Influence of interaction softness on phase separation of active particles, Phys. Rev. E **103**, 052605 (2021).
[53] J. Irving and J. G. Kirkwood, The statistical mechanical theory of transport processes. IV. The equations of hydrodynamics, J. Chem. Phys. **18**, 817 (1950).
[54] R. Soto and R. Golestanian, Self-assembly of catalytically active colloidal molecules: Tailoring activity through surface chemistry, Phys. Rev. Lett. **112**, 068301 (2014).
[55] C. H. Meredith, P. G. Moerman, J. Groenewold, Y.-J. Chiu, W. K. Kegel, A. van Blaaderen, and L. D. Zarzar, Predator–prey interactions between droplets driven by non-reciprocal oil exchange, Nat. Chem. **12**, 1136 (2020).
[56] D. Saintillan, Dispersion of run-and-tumble microswimmers through disordered media, Phys. Rev. E **108**, 064608 (2023).
[57] T. Ihle, R. Kürsten, and B. Lindner, Asymptotically exact scattering theory of active particles with anti-alignment interactions, arXiv:2303.03357.
[58] T. Ihle, R. Kürsten, and B. Lindner, Scattering theory of non-Brownian active particles with social distancing, arXiv:2303.03354.